Publisher homepage: www.universepg.com, ISSN: 2707-4625 (Online) & 2707-4617 (Print)
https://doi.org/10.34104/ijmms.022.01070113
International Journal of Material and Mathematical Sciences
Journal homepage: www.universepg.com/journal/ijmms

Investigation of Structural with Electronic Properties of Methylammonium Lead Iodide Perovskite Using Density Functional Theory

Md. Abdullah Al Asad*

Department of Electrical and Electronic Engineering, Bangabandhu Sheikh Mujibor Rahman Science and Technology University, Gopalganj, Bangladesh- 8100.

*Correspondence: dr.asad.eee@gmail.com (Dr. Md. Abdullah Al Asad, Associate Professor, Department of Electrical and Electronic Engineering, Bangabandhu Sheikh Mujibor Rahman Science and Technology University, Gopalganj, Bangladesh- 8100).

ABSTRACT

Employing first-principles calculations based on density functional theory (DFT), we have investigated bulk properties as well as the functions of lattice parameter, unit cell volume calculations, displacement parameter, interatomic distance, internal bond angle of relevant atoms on the optimized structures where the dependences of k-point summation and cut-off energies with corresponding lattice parameter variations are not dominant. Optimized structure's property of orthorhombic $CH_3NH_3PbI_3$ has great similarities with the prevalent experimental and/or theoretical data and shows a direct band gap crystal with a minimum band gap 1.80 eV at the gamma symmetry point.

Keywords: $CH_3NH_3PbI_3$, DFT, Lattice parameter, Atomic structure, K-point, and Cut- off energy.

INTRODUCTION:

As a dye sensitized solar cells (DSCs), perovskite $CH_3NH_3PbI_3$ (methyl-ammonium lead triiodide) has been widely utilized for solar cell application (E D Indari1 *et al*., 2017). $CH_3NH_3PbI_3$ contains octahedral PbI_6 units within its perovskite crystal structure with the general formula ABX_3, where A is $CH_3NH_3^+$, B is Pb2+, and X is I^-. $CH_3NH_3PbI_3$ has several attractive features, such as low cost, tenable band gap (Wan-Jian Yin *et al.,* 2015) and strong optical absorption (Wan-Jian Yin *et al.,* 2014). In 1978, when Dr Klaus Weber, synthesized and characterized $CH_3NH_3PbI_3$, he found that each Pb^{2+} cation is coordinated to six I^- anions to form PbI_6, which are corner connected to each other form a three-dimensional Pb-I framework (D. Weber, 1978). Each $CH_3NH_3^+$ cation stays at the centre of four PbI_6, which interacts with 12 I^- anions (Tom Baikie *et al.,* 2013). The symmetry and structure of $CH_3NH_3PbI_3$ crystals are highly dependent on the temperature according to the report of previous experiments (Tom Baikie *et al.,* 2013). At low temperature, an orthorhombic phase with Pnma space group is found which may transform into a tetragonal structure (space group: I4/m) above 161.4 K. The cubic phase (space group: Pm-3m) is found when the temperature is higher than 330.4 K. For improving the symmetry at the higher temperature, the fast-dynamic movement of $CH_3NH_3^+$ cations within the Pb-I framework is needed. At low temperature, the location of $CH_3NH_3^+$ cations can only be determined experimentally in case of orthorhombic phase where the lattice constants in orthorhombic crystal vary little (Tom Baikie *et al*., 2013). In addition, a novel light harvester, which can greatly improve the solar-conversion efficiency of dye-sensitized solar cells based on organic/inorganic hybrid $CH_3NH_3PbI_3$ perovskite.

The highest reported power conversion efficiency has increased from under 4% in 2009 (Akihiro Kojima *et al.,* 2009) to over 22% in recent years (Hanul Min *et al.,* 2021). The ability to tune the band gap

and related key properties of $CH_3NH_3PbI_3$ by doping the ions of various sub-lattices has been demonstrated in huge number of recent studies which broadens the optoelectronics applications (Keith P *et al*., 2018).

$CH_3NH_3PbI_3$ has already been accepted as a potential material for next-generation solar cell. To know the molecular design of organic/inorganic perovskite materials with defined properties, it is obvious to study the structures and chemistries of these prototype light harvesters. Among different perovskite formulations used in solar cells, $CH_3NH_3PbI_3$ is the most widely studied (Shenghao Wang *et al.,* 2016). As a result, our investigation is focused on the orthorhombic perovskite $CH_3NH_3PbI_3$. By ab initio calculations we have investigated both of structural and electronic properties of organic/ inorganic hybrid perovskite $CH_3NH_3PbI_3$ crystals. Density functional theory (DFT) is employed as it offers an efficient, yet accurate quantum mechanical method for theorists to optimize structures and determine energies of reactants and products (J. Even *et al,* 2014). In this letter, we present a theoretical investigation of structural with electronic properties of the orthorhombic phase of $CH_3NH_3PbI_3$. Different parameters are computed such as the lattice para-meters, the interatomic distances, the total energy, density of states with corresponding band structures and so on.

All these parameters are computed without considering any physicochemical effect. Afterwards, all results are compared with the available experimental data which are the important parameters for enhancing the electron transport and efficiency. In addition to that, it also leads the research in the exploration of material properties of high efficiency photovoltaics, high coefficient of the optical absorption, excellent charge carrier transportation, material stability and so on.

Computational Parametrization

Ab initio calculations are performed in the framework of the DFT, based on plane-wave basis set for the expansion of the single-particle Kohn-Sham wave functions and pseudopotentials. Electron-ion interactions are described using plane wave ultrasoft pseudopotentials with a kinetic energy cut-off of 520.0 eV. The Perdew-Burke-Ernzerhof (PBE) parametrization of the Generalized Gradient Approximation (GGA) (John P. Perdew *et al.,* 1997) is employed for the evaluation of the exchange-correlation energy under electronic and ionic self-consistence, with convergence criteria of 10^{-4} eV and -10^{-3} eV·Å^{-1}, respectively. Electron in valence states contained the Pb 6s, 6p, and 5d states, I 5s and 5p states, C 2s and 2p states, N 2s and 2p states, and the H 1s states. All atoms are relaxed after optimized their geometry where cell optimization technique is employed to optimize the lattice constants. For the calculations of structural with electronic properties, we perform Brillouin-zone integrations using Monkhorst-Pack grids of special points with (4×4×4) mesh. We reproduced the experimentally verified simple orthorhombic MAPI super cell that consists of perovskite units (a = 8.836Å, b = 12.580Å, c = 8.555Å) at low temperature (Tom Baikie *et al.,* 2013). The orthorhombic supercell of $CH_3NH_3PbI_3$ includes 48 atoms. DFT methods have been implemented in the Vienna Ab initio Simulation Package (version 5.4.1) (Jürgen Hafner, 2008) for ground state calculations.

The GGA-PBE calculation is performed for bulk of $CH_3NH_3PbI_3$ without incorporating spin-orbit coupling (SOC) effect to the DFT methods. As it is not possible to compute the contributions to the energy, forces, and stresses for an infinite number of cell replica, a tolerance parameter defining the number of cells to be considered is used in the DFT. Here, the Gaussian smearing is used and the stopping criterion on the residual of the forces on each atom is set to 10^{-7} eV·Å^{-1}, for the geometry optimizations.

RESULTS AND DISCUSSION:

Structural properties

To evaluate the performance of various functional, the of organic/inorganic hybrid perovskite $CH_3NH_3PbI_3$ crystal structures are firstly optimized where lattice parameters must be released numerically. This is done by allowing the atoms to move in a way that minimizes the forces present in the cell. The structure relaxation allows the determination of the atomic positions at the equilibrium. The initial lattice constants and the system of atomic coordinates in orthorhombic $CH_3NH_3PbI_3$ crystals for theoretical optimizations are from the X-ray diffraction (XRD) experiments at 100K (Tom Baikie *et al.,* 2013).The optimized lattice constants included with volumes using the various functional are listed into **Table 1** with the available experimental values (Tom Baikie *et al.,* 2013; Mostari *et al*., 2020).

Table 1: Computed lattice parameters included with unit cell volume are calculated by Perdew-Burke-Ernzerhof (PBE) parametrization, compared with experimental data (Tom Baikie *et al.,* 2013).

$CH_3NH_3PbI_3$	a (Å)	b (Å)	c (Å)	V(Å^3)
PBE/GGA	9.223	12.860	8.633	1024.06
Exp. [5]	8.836	12.580	8.555	951.01

Our results are in good agreement with experimental results. The relative error with respect to the experimental value for lattice constants does not exceed 5% where the total volume of unit cell becomes 7 % larger than the experimental results (Tom Baikie *et al.,* 2013). The optimized orthorhombic atomic structure, $CH_3NH_3PbI_3$ crystals using the PBE/GGA functional is shown in **Fig. 1**.

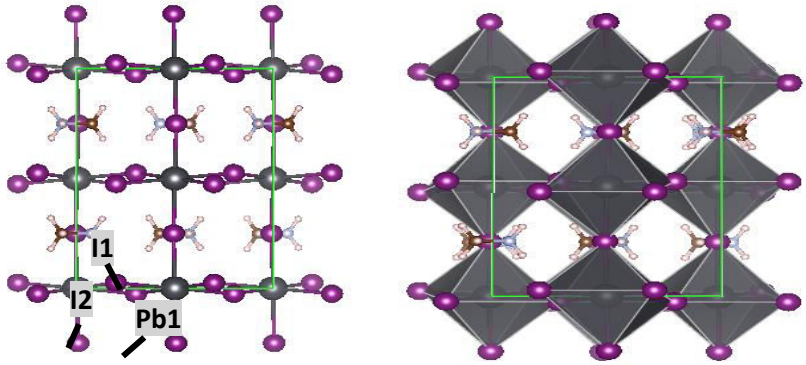

Fig. 1: The orthorhombic atomic structures of perovskite $CH_3NH_3PbI_3$ crystals without (left) or with (right) showing the [PbI_6] octahedra. Key: grey- Pb, purple- I, light blue- N, brown- C, and pink- H. Green solid line indicates the unit cell area.

The reduced coordinates of each atom are also modified due to the relaxation. The orthorhombic symmetry is still conserved. In relaxed system, the total energy is found to be equal to -203.8332 eV. In ideal crystallographic description, I^- anions show the transverse displacement from the mid-point of the Pb-Pb distance within [PbI_6] octahedral structures in XRD refinement experiments (**Fig. 1**). By using PBE functional relevant with experimental data, **Table 2** lists the theoretical displacement parameters: Pb1, I1 and I2 atoms, marked in **Fig. 1**. The atomic fractional coordinates between optimized and ideal crystallographic structures in displacement parameters are the main differences of them. Without the displacement of I1 atoms along a direction and I2 atoms along b direction, the overall theoretical displacement parameters show well agreement with the experimental values. The I2 atom shift better along both a, b directions but I2 atoms displacement in c directions are smaller than those of the I1 atoms.

Table 2: Displacement parameters for Pb1, I1 and I2 atoms of orthorhombic $CH_3NH_3PbI_3$.

Atoms	Functional	U_x	U_y	U_z
Pb1	PBE	0.000	0.000	0.000
	Exp. [5]	0.007	0.003	0.009
I1	PBE	0.007	0.000	0.012
	Exp. [5]	0.019	0.002	0.018
I2	PBE	0.008	0.007	0.004
	Exp. [5]	0.016	0.021	0.014

The optimized Pb-I bond length calculated with PBE is 3.26Å while the C-H, N-H and C-N bond lengths are 1.09, 1.04, and 1.49Å, respectively which are satisfied with the experimental values of 3.18, 1.1, 1.0, and 1.57Å (Tom Baikie *et al.,* 2013). The apical (along the b axis) and equatorial (along the c axis) Pb-I-Pb angles are respectively equal to 159.88 ^{o} and 152.78 ^{o} and compare well with the standard values of 161.9 ^{o} and 150.7 ^{o} (Tom Baikie *et al.,* 2013). All the results concerning the interatomic distances and the internal bond angles are listed in below **Table 3**. The Pb-I1-Pb angle is about 159^o in our PBE results, which is 7^o larger than the Pb-I2-Pb angle. These structural differences mark that I1 and I2 atoms are

inequivalent atoms. These parameters are all within 5% from the corresponding experimental values (Tom Baikie *et al.,* 2013).

Table 3: The optimized interatomic distances and internal bond angles among organic and inorganic atoms of $CH_3NH_3BbI_3$, verification with the experimental data.

Bonds [Å] Angle [^{o}]	PBE	EXP [5]
C-H	1.09	1.1
N-H	1.04	1.0
C-N	1.49	1.57
Pb-I	3.26	3.18
Pb-I-Pb (apical)	159.88 ^{o}	161.9 ^{o}
Pb-I-Pb (equatorial)	152.78 ^{o}	150.7 ^{o}

To investigate the dependence of k-point summation and cut-off energies, we have optimized the structure with various k-points grid and cut-off energies for obtaining corresponding lattice parameter variations. We found the maximum lattice constant difference is less than 0.25% for cut off energy variation in x direction and the angular change of them are not exceed 0.05% for both of k-point summations and cut off energy variations in x direction. The standard values of the cut-off energy for calculating other compounds from some literatures such as 400 eV/ 500 eV. In our system includes Pb ions which carry d electrons that have high localizations requiring higher cut-off energy, because the cut-off energy is related to minimum wavelength of electrons in/near the ionic core. Moreover, we noticed the dynamic movement of organic part, $CH_3NH_3^+$ cations with in the Pb-I framework is negligible and the internal structural change is not dominant. By increasing the k-point summations and cut off energy, a bit of dependence is observed, thus, chosen a set of minimum k-points summation, 4 x 4 x 4 and cut off energy, 520 eV is sufficiently enough for structural properties analysis if the cell size become in large. The data for optimized structure with k-point grid and cut off energy variations are shown in **Table 4**.

Table 4: The lattice parameters variations with k-point summations and cut off energies.

Cutoff Energies / K-point Summations	520 (eV)			600 (eV)		
	Lattice parameters					
	a[Å]	b[Å]	c[Å]	a [Å]	b[Å]	c [Å]
	α[degree]	β[degree]	γ[degree]	α[degree]	β[degree]	γ[degree]
4 x 4 x 4	9.22333	12.86079	8.63317	9.24627	12.86462	8.63007
	89.99°	90.00°	90.00°	89.98°	90.00°	90.00°
6 x 6 x 6	9.22147	12.86184	8.63220	9.24009	12.86970	8.62316
	89.98°	89.99 °	90.00°	89.94°	90.00°	90.00°

Electronic properties

The crucial factors of organic/inorganic hybrid $CH_3NH_3PbI_3$ materials are the electronic structures where the sunlight absorption used as light harvesters in DSCs (Julian Burschka *et al.,* 2013).The bandgap energy is estimated 1.80 eV calculated from total density of states (TDOS) using the PBE/GGA functional (see **Fig. 2**) where the experimental lattice constants were used (Tom Baikie *et al.,* 2013). The structural properties have the great impact on bandgap energies and highlight the significance of using approximations which accurately reproduce the correct geometry (Ivo Borriello *et al.,* 2008). By employed optB86b+vdWDF functional (J. Even *et al.,* 2014), the theoretical bandgap energy is 1.74 eV which is 0.06 eV smaller than PBE functional. This difference can be focused on the various theoretical lattice constants taken by various functional. At low temperature (Ishihara T, 1994)] in optical absorption experiments, the electronic bandgap is 1.68 - 1.72 eV in case of orthorhombic $CH_3NH_3PbI_3$ crystals. Although, the theoretical predictions at the non-local and sami-local level of bandgap energies of hybrid $CH_3NH_3PbI_3$ are almost close to the experimental values, but in some case, the bandgap energies deviation of solid-state semiconductors is about 30% (Haijun Yu et *al.,* 2012) by using DFT functional. This is why good band gaps are not normally to be expected from functional of the types tested here. To know the band structure of $CH_3NH_3PbI_3$ is interesting as it gives information about the electronic transition. Representing the 3D grid band structure of the Brillouin zone is impossible as it requires a four-dimensional plot. A more convenient way to represent it consists in defining paths along high symmetric directions. The acquirement of a band structure is a two-step process. Firstly, the density must be obtained thanks to a self-consistent calculation.

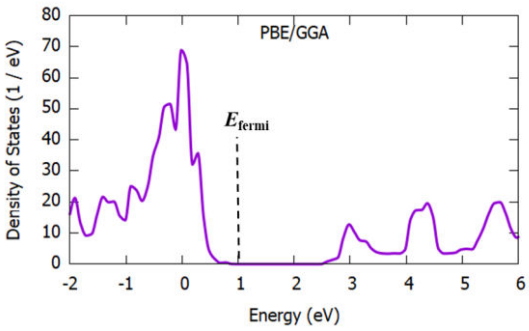

Fig. 2: Total density of states (TDOS) for orthorhombic CH3NH3PbI3 crystals and its bandgap energy using PBE/GGA functional.

Secondly, the density used when solving the Kohn-Sham equation for many different k points, along the defined paths in Brillouin zone. It ensures that the potential will not vary during the scan of different k point's lines. The Brillouin zone of the orthorhombic cell is represented as in **Fig. 3**. Let's consider the following directions of high symmetry: Γ→ Z→T →Y→S →X→U→R.

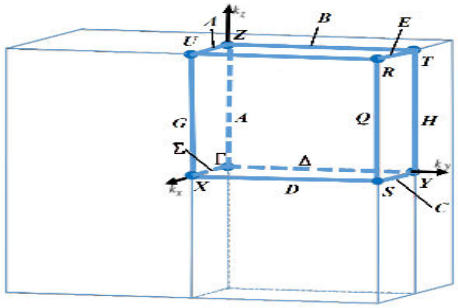

Fig. 3: Scheme of the Brillouin Zone for an orthorhombic lattice. Where Γ (0.0,0,0); Z (0,0,1/2); T (0.0,1/2,1/2); Y (0.0, 1/2,0); S (1/2, 1/2,0); X (1/2,0.0,0); U (1/2,0.0, 1/2); R (1/2, 1/2, 1/2) are respective coordinates.

The electronic band structure (depicted at the converged parameters) is represented in **Fig. 4**. Upper lines than fermi energy level are conduction bands while lower ones are valence bands. The orthorhombic phase of $CH_3NH_3PbI_3$ shows a direct band gap occurring at the point (0, 0, and 0) which is the highest symmetrical point of the Brillouin zone. The estimated band gap is almost equal to ⇠1.80 eV. In general, when using LDA or GGA calculation methods, the band gap energy is often underestimated which is famous DFT band-gap problem. This effect probably comes from the fact that the spin-orbit coupling is not considered. Thus, the priorities of SOC in the DFT calculation has been pointed out (Jacky Even *et al.*, 2013). The harmony with the experimental result degrades seriously if this interaction is incorporated into the DFT calculation within PBE or the local-density approximation and the E_g reduces significantly down to 0.5 eV (Giacomo Giorgi *et al.* 2013).

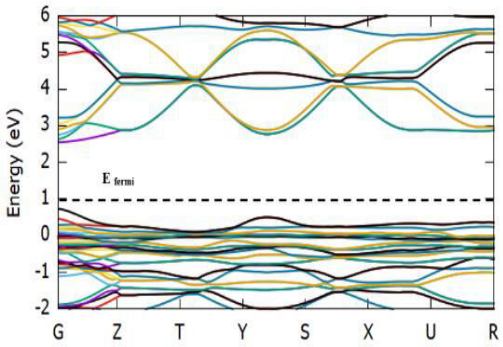

Fig. 4: Band structure of the orthorhombic cell for specific symmetries directions in the Brillouin zone: Γ-Z-T -Y-S -X-U-R. Dash line represented the fermi energy level. A band gap of 1.80eV is found.

When the SOC effect is considered using the GW approximation (Paolo Umari *et al.,* 2014) or a hybrid functional (E. Menéndez-Proupin *et al.,* 2014), the experimental E_g of 1.6 eV can be reproduced. However, the band structures obtained from these sophisticated calculations are essentially like that deduced from the simple PBE calculation (Wan-Jian Yin *et al.,* 2015). Therefore, the PBE calculation is performed without incorporating the SOC effect.

CONCLUSION:

In summary, first-principle DFT calculations were performed to study structural with electronic properties of orthorhombic perovskite $CH_3NH_3PbI_3$ materials. Our results concluded that the optimized lattice constants using PBE/GGA does not exceed 5%, compared to the experimental value and the displacement parameters included interatomic distances with internal bond angles satisfy the experimental results. The chosen set of minimum k-points summation, 4 x 4 x 4 and cut off energy, 520 eV is sufficiently enough for structural properties analysis if the cell size becomes in large. The electronic properties analysis concluded that orthorhombic CH_3 NH_3 PbI_3 exhibits as a direct band gap crystal with minimum band gap is about 1.80 eV at the gamma symmetric point.

ACKNOWLEDGEMENT:

I'm grateful to all the dear Professors for providing their information regarding this research.

CONFLICTS OF INTEREST:

The author of this manuscript declares agreement with the statements and has no conflicts of interest.

REFERENCES:

1) Akihiro Kojima, Yasuo Shirai and Tsutomu Miyasaka, (2009). Organometal Halide Perovskites as Visible-Light Sensitizers for Photovoltaic Cells, *Am. Chem. Soc*, **131**, 6050-6051. https://pubs.acs.org/doi/10.1021/ja809598r
2) D. Weber, (1978), CH3NH3PbX3, a Pb (II)-System with Cubic Perovskite Structure, *Zeitschrift für Naturforschung B,* **33**, 1443-1445. https://www.degruyter.com/document/doi/10.1515/znb-1978-1214/html?lang=de
3) E. Menéndez-Proupin, P. Palacios, P. Wahnón, and J. C. Conesa, (2014). Self-consistent relativistic band structure of the CH3NH3PbI3 perovskite, *Phys. Rev. B*, **90**, 045207. https://journals.aps.org/prb/abstract/10.1103/PhysRevB.90.045207
4) E D Indari1, T D K Wungu 2 and R Hidayat. (2017). Ab-Initio Calculation of Electronic Structure of Lead Halide Perovskites with Formamidinium Cation as an Active Material for Perovskite Solar Cells, *J. of Physics*: Conf. series, **877** (012054). https://iopscience.iop.org/article/10.1088/1742-6596/877/1/012054/meta
5) Giacomo Giorgi, Hiroshi Segawa, and Koichi Yamashita, (2013). Small Photocarrier Effective Masses Featuring Ambipolar Transport in Methylammonium Lead Iodide Perovskite: A Density Functional Analysis, J. *Phys. Chem. Lett.* **4,** 4213. https://pubmed.ncbi.nlm.nih.gov/26296167/
6) Hanul Min, Do Yoon Lee, Tae Joo Shin & Sang Il Seok, (2021). Perovskite solar cells with atomically coherent interlayers on SnO2 electrodes, *Nature* **598**, 444-450. https://www.nature.com/articles/s41586-021-03964-8
7) Haijun Yu, Ping He, Yumiko Nakamuraa and Haoshen Zhou, (2012). High-energy 'composite' layered manganese-rich cathode materials via controlling Li2MnO3 phase activation for lithium-ion batteries, *Phys. Chem. Chem. Phys.,* **14,** 23332338. https://pubs.rsc.org/en/content/articlelanding/2012/cp/c2cp40745k
8) Ishihara, T., (1994). Optical properties of PbI-based perovskite structures, *J Lumen,* **60,** 269-274. https://ui.adsabs.harvard.edu/abs/1994JLum...60..269I/abstract
9) Ivo Borriello, Giovanni Cantele, and Domenico Ninno, (2008). Ab initio investigation of hybrid organic-inorganic perovskites based on tin halides, *Phys. Rev.* **B 77**, 235214. https://journals.aps.org/prb/abstract/10.1103/PhysRevB.77.235214
10) J. Even, L. Pedesseaua and C. Katanb, (2014), Comment on "Density functional theory analysis of structural and electronic properties of orthorhombic perovskite CH3NH3PbI3" by Y. Wang *et al.,* Phys. *Chem. Chem. Phys.,* **16**, 1424-1429. https://pubs.rsc.org/en/content/articlelanding/2014/cp/c3cp55006k
11) Jacky Even, Jean-Marc Jancu, and Claudine Katan, (2013). Importance of Spin - Orbit Coupling in Hybrid Organic/ In-organic Perovskites for Photovoltaic Applications. *J. Phys. Chem. Lett*. **4**, 2999. https://pubs.acs.org/doi/10.1021/jz401532q
12) John P. Perdew, Kieron Burke, and Matthias Ernzerhof, (1997). Generalized Gradient Approximation Made Simple, *Phys. Rev. Lett*., **77**, 3865-3868. https://journals.aps.org/prl/abstract/10.1103/PhysRevLett.77.3865
13) Julian Burschka, Nazeeruddin and Michael Grätzel, (2013). Sequential deposition as a route to high-performance perovskite-sensitized solar cells, *Nature,* **499**, 316-320. https://www.nature.com/articles/nature12340
14) Jürgen Hafner, (2008), Ab-initio simulations of materials using VASP: Density-functional theory and beyond, *J. Comput. Chem*.; **29**, 2044-2078. https://onlinelibrary.wiley.com/doi/abs/10.1002/jcc.21057
15) Keith P. McKenna, (2018). Electronic Properties of {111} Twin Boundaries in a Mixed-Ion Lead Halide Perovskite Solar Absorber, *ACS Energy Letter*, **3,** 2663-2668. https://pubs.acs.org/doi/10.1021/acsenergylett.8b01700
16) Mostari F, Rahman MA, and Khatun R. (2020). First principles study on the structural, elastic, electronic, and optical properties of cubic 'half-

Heusler' alloy RuVAs under pressure, *Int. J. Mat. Math. Sci*., **2**(4), 51-63. https://doi.org/10.34104/ijmms.020.051063

17) Paolo Umari, Edoardo Mosconi & Filippo De Angelis, (2014). Relativistic GW calculations on CH3NH3PbI3 and CH3NH3SnI3 Perovskites for Solar Cell Applications, *Sci. Rep*. **4**, 4467. https://www.nature.com/articles/srep04467

18) Shenghao Wang, Luis K. Ono & Yabing Qi (2016). Accelerated degradation of methylammonium lead iodide perovskites induced by exposure to iodine vapour, *Nat. Energy*, **2**, 16195. https://www.nature.com/articles/nenergy2016195

19) Tom Baikie, Michael Graetzel and Tim J. White, (2013). Synthesis and crystal chemistry of the hybrid perovskite (CH3NH3) PbI3 for solid-state sensitised solar cell applications, *J Mater Chem, A*, **1**, 5628-5641. https://pubs.rsc.org/en/content/articlelanding/2013/ta/c3ta10518k

20) Wan-Jian Yin , Tingting Shi, and Yanfa Yan, (2014). Unique properties of halide perovskites as possible origins of the superior solar cell performance, *Adv Mater*, **26** (27), 4653-8. https://pubmed.ncbi.nlm.nih.gov/24827122/

21) Wan-Jian Yin, Joongoo Kang, Yanfa Yanand Su-Huai Wei, (2015). Halide perovskite materials for solar cells: a theoretical review, *J. of Materials Chemistry A,* **3**(17), 8926-8942. https://pubs.rsc.org/en/content/articlelanding/2015/ta/c4ta05033a

Citation: Asad MAA. (2022). Investigation of structural with electronic properties of methylammonium lead iodide perovskite using density functional theory, *Int. J. Mat. Math. Sci.*, **4**(6), 107-113. https://doi.org/10.34104/ijmms.022.01070113